Mobility of Basal Dislocations in Zinc

D. P. Pope+ and T. Vreeland, Jr.

W. M. Keck Laboratories, California Institute of Technology
Pasadena, California

ABSTRACT

This paper reports the results of an experimental study in which basal dislocation velocities were measured in zinc as a function of stress, temperature and dislocation orientation. The velocities were measured using the direct or Gilman-Johnston technique in which the individual dislocations themselves are observed. Tests were performed on 99.999% purity monocrystals. The applied resolved shear stress ranged from 0 to about 20×10^6 dynes/cm^2, the load durations were in the microsecond range, the test temperatures were 300, 223, 173 and 123°K, and the measured velocities ranged from about 200 to 2000 cm/sec. Since the velocities are a linear function of stress and the velocity at a given stress increases with decreasing temperature, the velocity controlling mechanism is believed to be an interaction between the moving dislocations and the thermal waves of the lattice. The phonon viscosity and the phonon scattering mechanisms are compared to the data.

+ Present address, School of Metallurgy and Materials Science and Laboratory for Research on the Structure of Matter, University of Pennsylvania, Philadelphia, Pennsylvania.

1. INTRODUCTION

In a previous paper (Pope, Vreeland and Wood 1967) it was reported that the velocity of edge dislocations in the basal system of zinc is a linear function of stress at room temperature and that the constant of proportionality agrees reasonably well with that for a dislocation-phonon interaction mechanism. On the basis of this data the authors stated that a phonon interaction probably was the velocity-controlling mechanism but a final conclusion could not be made until tests were made at various temperatures. If a phonon mechanism is operative, then the velocity at a constant stress should increase when the temperature is decreased and the sense of this dependence is unique to phonon interactions. All other velocity controlling mechanisms lead to an increasing velocity with increasing temperature at constant stress. Gorman, Wood and Vreeland (1969) and (1969) have recently reported that a dislocation-phonon interaction mechanism is the velocity controlling mechanism in aluminum at low temperatures. This is the only other reported direct velocity measurement on any material in which such an effect has been observed. The purpose of the present work was to determine the temperature dependence of basal dislocation velocities in zinc and decide from the sense of the dependence whether a phonon mechanism is operative.

In the work reported earlier (Pope, Vreeland and Wood 1967) tests were carried out on 99.999% purity zinc single crystals of low

dislocation density. Edge dislocation velocities were measured by the Gilman-Johnston technique (Johnston and Gilman 1959) wherein the crystal is given a small amount of controlled local damage to produce fresh dislocations, the initial dislocation configuration is observed, a load pulse of known magnitude and duration is applied to the crystals and the dislocation configuration is again observed. The dislocation velocity is then the distance travelled divided by the pulse duration. The tests reported here were the same as the previous tests with the following exceptions: (1) Edge, screw and mixed dislocation velocities were measured as opposed to the previous work in which only edge velocities were measured. (2) Tests were carried out at 123, 173, 223 and 300°K. (3) The crystals in the present work were prepared with improved techniques which reduced the amount of substructure and the dislocation density.

The tests were conducted on specimens machined into right circular cylinders whose longitudinal axes were parallel to the crystallographic c axis and whose ends were parallel to basal planes. Dislocations were produced on one end of each specimen by scratching the surface with an Al_2O_3 whisker loaded with 50 mg. The scratched surface of the specimen was bonded to a loading fixture and a torsion pulse of 10 to 40 μ sec duration was applied to the specimen. The dislocation configuration before and after testing was observed by means of the Berg-Barrett x-ray technique.

2. TEST SPECIMEN PREPARATION

The test specimens were prepared in essentially the same manner as previously described (Pope, Vreeland and Wood 1967). Briefly the procedure is the following: Randomly oriented single crystals were grown from 99.999% purity material using the Bridgeman technique. Test specimens were cut from the bulk material by a combination of acid machining and cleaving techniques previously described. These specimens had at least one cleaved end which, after annealing, served as the test surface. Crystals were annealed at 370°C for 1/2 to 3 hours in an argon atmosphere. It was found that significant improvements in dislocation substructure density could be obtained by additional care in specimen preparation and that thermal etching of the test surface could be avoided by using an argon rather than a hydrogen atmosphere during the anneal. Consequently the quality of the crystals used in this study was better than those used in the tests reported earlier (Pope, Vreeland and Wood 1967).

3. EXPERIMENTAL TECHNIQUES

3.1 Method of Producing Dislocations to be Studied

Fresh dislocation were produced by scratching the basal plane test surface in a carefully controlled manner. The scratch geometry is as shown in fig. 1. Six diametrical scratches were made on each specimen, three along $\langle 1\bar{0}10 \rangle$ and three along $\langle 1\bar{2}10 \rangle$ directions. The two scratch directions produce dislocations oriented as shown in fig. 2.

Fig. 2a shows a scratch along $<1\bar{0}10>$ and it produces dislocations with Burgers vectors perpendicular to the scratch line. Therefore segments along ℓ_1 are of edge orientation and segments along ℓ_2 are of screw orientation. The exact manner in which the dislocations arrange themselves around the scratch tip is unknown and therefore that part of fig. 2a is an idealization. This uncertainty arises because in this vacinity of the scratch the dislocations are too close together to be individually resolved in the BB photograph. However, since the dislocations cannot terminate in the crystal, the lines must curve back on themselves near the scratch tip, producing a screw oriented segment. Edge dislocation displacements were measured perpendicular to a radius of the specimen while screw dislocation displacements were measured parallel to a radius.

The dislocation configuration around a scratch parallel to $<1\bar{2}10>$ is shown in fig. 2b. In this case the scratching process produces dislocations with two sets of Burgers vectors, $\pm b_1$ and $\pm b_2$. Only the displacement of segment ℓ_1 was measured on these scratches since segment ℓ_2 on these was also of mixed character. It should be noted here that since both $\pm b_1$ and $\pm b_2$ make an angle of 30° with the applied stress both experience the same resolved shear stress.

3.2 X-Ray Technique and Loading System

The Berg-Barrett (BB) method is described by Schultz and Armstrong (1964) and by Pope, Vreeland and Wood (1967) as applied to observing basal dislocations in zinc. The techniques and equipment

used in the present study are described by Turner, Vreeland and Pope (1968). The BB technique is particularly useful for this application because it allows the determination of the direction (but not the sense) of the Burgers vector of an individual dislocation. Therefore the stress resolving factor was known for all dislocations whose displacements were measured in this study.

The loading system has been described elsewhere (Pope, Vreeland and Wood 1964) and was used as described by Pope, Vreeland and Wood (1967), Greenman, Vreeland and Wood (1967) and Gorman, Wood and Vreeland (1969).

3.3 Specimen Bonding Techniques

A new room temperature bonding technique was developed that was less complex than the one described earlier. This technique consisted of heating the mating part of the loading system to 75°C, coating it with a low melting point wax and pressing the specimen against the soft wax. This resulted in a joint which passed the stress pulse at 300°K without distorting it and yet did not damage the specimen during solidification. Bonding agents for the low temperature tests were made using mixtures of ethanol and glycerine as described by Gorman, Wood and Vreeland (1969).

4. EXPERIMENTAL RESULTS

4.1 Dislocation Displacements

Fig. 3 shows enlargements of two different portions of a BB photograph of a specimen tested at 223°K. 0.43 cm. of the 0.55 cm

specimen radius is shown in the figure. Fig. 3a shows dislocations around $<1\bar{0}10>$ type scratches and therefore edge and screw displacements are measured here. Fig. 3b shows dislocations around a $<1210>$ type scratch and mixed dislocation displacements are measured here. The dislocation displacements are seen to be a linear function of radius in this figure. Since the specimen is loaded in torsion, the shear stress on a basal plane is given by

$$\tau = \tau_{max}(r/R)$$

where τ_{max} is the stress at the maximum radius, R, and r is the distance from the specimen center. For the edge and screw dislocations the resolved shear stress is equal to the applied stress while for the mixed dislocations the resolved stress is $\tau \cos 30^\circ$.

Since the stress is linear with radius and the dislocation displacements are also linear with radius (as can be seen in fig. 3b), it is clear that the velocity is a linear function of stress. This was found to be true at all temperatures.

4.2 Dislocation Velocities

Fig. 4 shows plots of velocity vs. stress for edge dislocations at all test temperatures. Fig. 5 shows the same for mixed dislocations and fig. 6 shows the plots at 173 and 300°K for screw dislocations. The lack of screw velocity data at the other test temperatures is due to several factors. As shown in fig. 1, screw dislocations are only produced at the ends of scratch segments and therefore there were relatively short lengths initially present on a

specimen. Also many of them either appeared to be pinned (immobile) or they seemed to have cross slipped out of the specimen.

The damping constant, B, is defined by the equation, $\tau_r b = Bv$ where τ_r is the resolved shear stress, b is the magnitude of the Burgers vector, and v is the velocity. The relationship between τ_r and v is obtained from figs. 4, 5, and 6 by drawing a line from the origin through the average of the experimental points. Fig. 7 shows plots of B vs. temperature for edge, screw and mixed dislocations. It can be seen in this figure that B decreases quite rapidly with decreasing temperature for all three dislocation types and therefore the velocity at a given stress must be increasing with decreasing temperature. As stated earlier in this paper this is the type of temperature dependence that is expected from a dislocation-phonon type interaction mechanism.

5. DISCUSSION

Velocity and stress can be measured in this experiment to within ±10% and ±5% respectively. This still does not account for the magnitude of the scatter seen in figs. 4, 5 and 6. Possible sources of the scatter are discussed below.

5.1 Effect of Line Tension

As stated previously (Pope, Vreeland and Wood 1967) line tension cannot be a significant source of error except at the scratch tips where the dislocation curvature is large. Therefore this effect would mainly influence the screw, and might be part of the reason for the small number of screw dislocation displacements.

5.2 Dislocation Interactions

The basal dislocations are initially spaced about 6×10^{-4} cm apart around the scratch before application of the load pulse. This spacing could lead to a significant interaction stress compared to the applied stress. However, they are much more widely spaced after the test and therefore we conclude that during most of the motion interactions are negligible. The basal dislocations can also interact with the nonbasal forest, an interaction that is known to be quite large (Stofel and Wood 1963). The forest density of these crystals is about 10^3 to $10^4 cm^{-2}$ which could contribute significantly to the scatter. It is believed that this is probably the reason why the average room temperature dislocation velocities reported earlier (Pope, Vreeland and Wood 1967) were lower than those reported here. The improved preparation techniques used in this study would reduce the forest density as well as the substructure and probably result in higher velocities.

5.3 Pinning by Point Defects

While we had very little control over the exact concentration of point defects every attempt was made to minimize their number by using high purity material and a clean annealing atmosphere. We also minimized the aging time between scratching and testing.

5.4 Acceleration Times

The time required for a dislocation to accelerate to its terminal velocity must be small compared to the load pulse duration for the

average velocity to be essentially the terminal velocity. For a dislocation moving under the influence of an applied stress τ in a viscous medium the velocity as a function of stress and time is given by:

$$v = \frac{\tau b}{B}\left(1 - e^{-\frac{Bt}{m}}\right) .$$

B is the drag coefficient of the viscous medium, b is the magnitude of the Burgers vector, t is time after stress application and m is $\frac{Gb^2}{c^2}$ where G is the shear modulus and c is the shear wave velocity. At time $t = m/B$ the velocity differs from the terminal velocity by 1/e. For this case $m/b = 10^{-11}$ sec which is indeed small compared to the stress pulse duration and therefore acceleration times can be neglected.

Of the various sources of scatter considered above, only interaction with other basal dislocations could increase the dislocation velocity. As these interactions are believed to be small, it appears that the true stress-velocity relationship for a basal dislocation in an otherwise perfect crystal lies above the average value shown in Figs. 4, 5 and 6. Further confirmation of this is found by comparison of the room temperature data of Pope, Vreeland and Wood (1967) with that observed in this study. The scatter in the earlier study was greater, with the maximum velocity values nearly the same as in the present study, but the average values were less (a damping constant of 8×10^{-4}

dynes- sec-cm^2 was reported, while the average values of the present data give 5×10^{-4} cgs.) This is attributed to more nearly perfect crystals as stated earlier in this paper.

Table I lists values of B taken from the average and the maximum velocity data. The values of B based on the average velocities are about 25% above the values based on the maximum velocities.

Temp.	Edge		Screw		Mixed	
	B_1	B_2	B_1	B_2	B_1	B_2
300	5.0	3.5	3.7	3.4	4.8	3.4
223	4.4	3.3	-	-	3.9	3.2
173	3.4	2.5	2.7	2.1	2.9	2.2
123	2.8	2.2	-	-	2.7	2.1

Table 1. Comparison of damping constants obtained from average and maximum velocities in figs. 4, 5 and 6. B_1 is obtained from the average velocities and B_2 is obtained from the maximum velocities. Units are °K and dyn-sec-cm^{-2}.

5.5 Comparison with Theoretical Models

In this section only those models which predict a linear velocity stress dependence and a velocity at constant stress which increases with decreasing temperature will be discussed. This clearly eliminates from consideration all mechanisms which depend on thermal activation such as dislocation interactions with point defects (Johnston and Gilman 1959, Fleischer 1962) Peirels barriers (Dorn and Rajnak 1964) and forest

dislocations (Seeger, Mader and Kronmuller 1963), because these predict a rapidly increasing velocity with increasing temperature. Therefore, we can restrict our consideration to those models which consider dislocation interactions with lattice thermal waves and with electrons, i.e., the intrinsic resistance of the perfect crystal itself to the motion of dislocations.

Three distinct phonon interaction mechanisms with low velocity dislocations have been discussed in the literature (velocities small compared to sonic velocities). Phonon interaction with the moving strain field of the dislocation (Sections 5.5.1 and 5.5.2 below) 2) Anharmonic radiation from the dislocation core (Section 5.5.3 below) and 3) Phonon induced flutter of the dislocation line (Section 5.5.4 below). Electron-dislocation interactions are considered in Section 5.5.5.

5.5.1 Phonon Viscosity

One theory of phonon interaction with the moving stress field is due to Mason (1960), (1964) and Mason and Bateman (1964). This phonon viscosity model treats the local equilibration of phonon modes, while the thermoelastic effect (Section 5.5.2) treats the damping due to heat flow.

The phonon viscosity model predicts a damping constant

$$B = \alpha \frac{b^2 D E_o K}{a^2 C_v U^2}$$

where α is constant depending on dislocation orientation, b is the Burgers vector, D is a non-linearity constant, E_o is the thermal

energy density, K is the lattice thermal conductivity, a is the dislocation core radius, C_v is the specific heat at constant volume, and U is the mean phonon velocity. α is given by

$$\alpha_{edge} = \frac{3}{32\pi(1-\nu)}$$

$$\alpha_{screw} = \frac{1}{8\pi}$$

where ν is Poisson's ratio. D is a constant whose magnitude is difficult to determine in the absence of third order elastic constant measurements but whose order of magnitude is 1.

When B is calculated at room temperature (see Ferguson, Hauser and Dorn 1967) a value of about 10^{-4} dyn sec cm^{-2} is obtained. This is the same order of magnitude as observed in these experiments. Also as seen in Table I, B for edge dislocations is higher than that for screw dislocations and the values for mixed dislocations are in between as the theory would predict. The numerical values of B from this theory should not be expected to be better than an order of magnitude estimate at any temperature due to uncertainties in a and D. The predicted and observed values of B_2 are plotted in Fig. 8 where the damping constants are normalized to the value at 300°K to facilitate the comparison of the relative temperature dependencies.

5.5.2 Thermoelastic Effect

Eshelby (1949) proposed a model in which a dislocation is damped by irreversible heat flow between regions of compressive and tensile stress. Lothe (1962) showed that in a metal this effect gives rise to

a much smaller drag coefficient than that observed in these experiments.

5.5.3 Anharmonic Radiation from the Dislocation Core

As a dislocation moves through the lattice, the atoms in the dislocation core are displaced relative to each other such that their vibrations become anharmonic. Lothe (1962) has calculated the drag coefficient that would result from this type of interaction and it appears to be too small to explain the present results at 300°K, and the predicted B appears to decrease more rapidly with temperature than the experimental values.

5.5.4 The Flutter Mechanism

In the flutter mechanism, the dislocation is treated as a vibrating line which absorbs and re-radiates phonons (Leibfried, 1950). This model gives about the correct magnitude of B at room temperature, and its temperature dependence is shown in Fig. 8.

5.5.5 Electron Interactions with Dislocations

The free electrons in a metal can also cause dislocation damping (Mason 1958, Elbaum and Hikata 1968, Huffman and Louat 1968). However, this effect should not be significant above 100°K.

5.5.6 The Total Drag

The total drag in the present experiments may be the sum of the drags resulting from phonon viscosity and flutter interactions. While theoretical estimates of the relative magnitudes of the two interactions

are inconclusive as to which is dominant, a comparison of their temperature dependencies with the experimental observations might resolve the question. Figure 8 shows that the normalized B_2 values follow a temperature dependence more nearly equal to that of the phonon viscosity theory. This indicates that the phonon viscosity effect may dominate, but the experimental values are not sufficiently precise to rule out the possibility of a nearly equal contribution from both mechanisms.

5.6 Comparison with Other Experimental Results

Ferguson, Hauser and Dorn (1967) measured the stress dependence of strain rate for high strain rates at temperatures from 300 to 653°K. They found that in zinc the plastic shear strain rate $\dot{\gamma}$ is proportional to the resolved stress minus a back stress τ_b and is independent of temperature. Thus

$$\alpha\dot{\gamma} = \tau - \tau_b = \alpha\rho bv$$

Taking $(\tau - \tau_b)b = Bv$, implies that $B = \alpha\rho b^2$. Assuming that ρ is a constant, namely $10^8 cm^{-2}$ independent of stress and temperature, they find B is 3.5×10^{-4} dyn sec cm^{-2} and is temperature independent in the range studied. However, τ_b as defined above is found to be 30×10^6 dyn cm^{-2}. Thus the stress at which Ferguson et al. would observe zero strain rate at room temperature is about equal to the highest stress used in the present study at which the dislocation velocity was measured to be about 1500 cm/sec. A high density of forest dislocations (due to slip on the second order pyramidal system) in the

crystals used by Ferguson et al. might explain this difference.

Yoshida and Nagata (1968) studied the deformation behavior of zinc crystals in static and dynamic compression tests. At a strain rate of $7 \times 10^{2} sec^{-1}$ specimens deforming by basal slip were found to exhibit increasing flow stress with increasing temperature over the temperature range 77^{o} to $400^{o}K$. From this they conclude that phonon drag controls the relationship between the strain rate and the flow stress at strain rates above 10 sec^{-1}. The results of the present investigation support their conclusion, and permit calculation of the density of moving dislocations in their experiments.

ACKNOWLEDGMENTS

The authors are indebted to K. H. Adams for his early work on this project and to G. R. May who prepared the test specimens.

This work was sponsored by the U. S. Atomic Energy Commission.

REFERENCES

Dorn, J. E., and Rajnak, S., 1964, Trans. AIME 230, 1052.

Elbaum, L., and Hikata, A., 1968, Phys. Rev. Letters, 20, 264.

Eshelby, J. D., 1949, Proc. Roy. Soc. (London) A197, 396.

Ferguson, W. G., Hauser, F. E., and Dorn, J. E., 1967, Brit. J. Appl. Phys. 18, 411.

Fleischer, R. L., 1962, J. Appl. Phys. 33, 3504.

Gorman, J. A., Wood, D. S., and Vreeland, Jr., T., 1969, J. Appl. Phys. 40, 833.

Gorman, J. A., Wood, D. S., and Vreeland, Jr., T., 1969, J. Appl. Phys. 40, 903.

Greenman, W. F., Vreeland, Jr., T., and Wood, D. S., 1967, J. Appl. Phys. 38, 3595.

Huffman, G. P., and Louat, N. P., 1968, Dislocation Dynamics (McGraw-Hill Book Co., New York), 756.

Johnston, W. G., and Gilman, J. J., 1959, J. Appl. Phys. 30, 129.

Leibfried, G., 1950, Z. Phys. 127, 344.

Lothe, J., 1962, J. Appl. Phys. 33, 2116.

Mason, W. P., 1958, Physical Acoustics and the Properties of Solids (D. Van Nostrand Co., Inc., Princeton), 323.

Mason, W. P., 1960, J. Acoust. Soc. Am. 32, 458.

Mason, W. P., and Bateman, T. B., 1964, J. Acoust. Soc. Am. 36, 644.

Mason, W. P., 1964, J. Appl. Phys. 35, 2779.

Pope, D. P., Vreeland, Jr., T., and Wood, D. S., 1964, Rev. Sci. Instr. 35, 1351.

Pope, D. P., Vreeland, Jr., T., and Wood, D. S., 1967, J. Appl. Phys. 38, 4011.

Schultz, J. M., and Armstrong, R. W., 1964, Phil. Mag. 10, 497.

Seeger, A., Mader, S., and Kronmuller, H., 1963, Electron Microscopy and Strength of Crystals (Interscience Publishers, Inc., New York), 665.

Stofel, E. J. and Wood, D. S., 1963, Fracture of Solids (Interscience Publishers, Inc., New York), 521.

Turner, A. P. L., Vreeland, Jr., T., and Pope, D. P., 1968, Acta Cryst. A24, 452.

Yoshida, S. and Nagata, N., 1968, Trans. Japan. Instit. Metals, 9, 110.

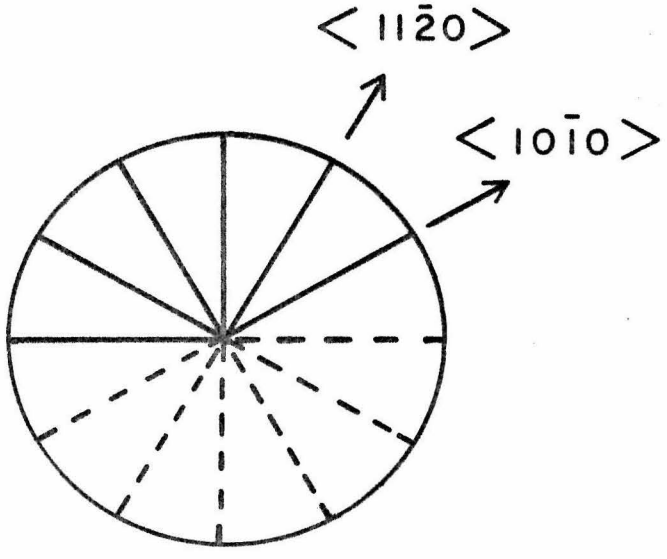

1. Scratch configuration on the basal plane. The <1 0 $\bar{1}$ 0> type scratches produce edge and screw dislocations while the <1 1 $\bar{2}$ 0> type scratches produce mixed dislocations. Some scratches were continuous, others were interrupted as shown.

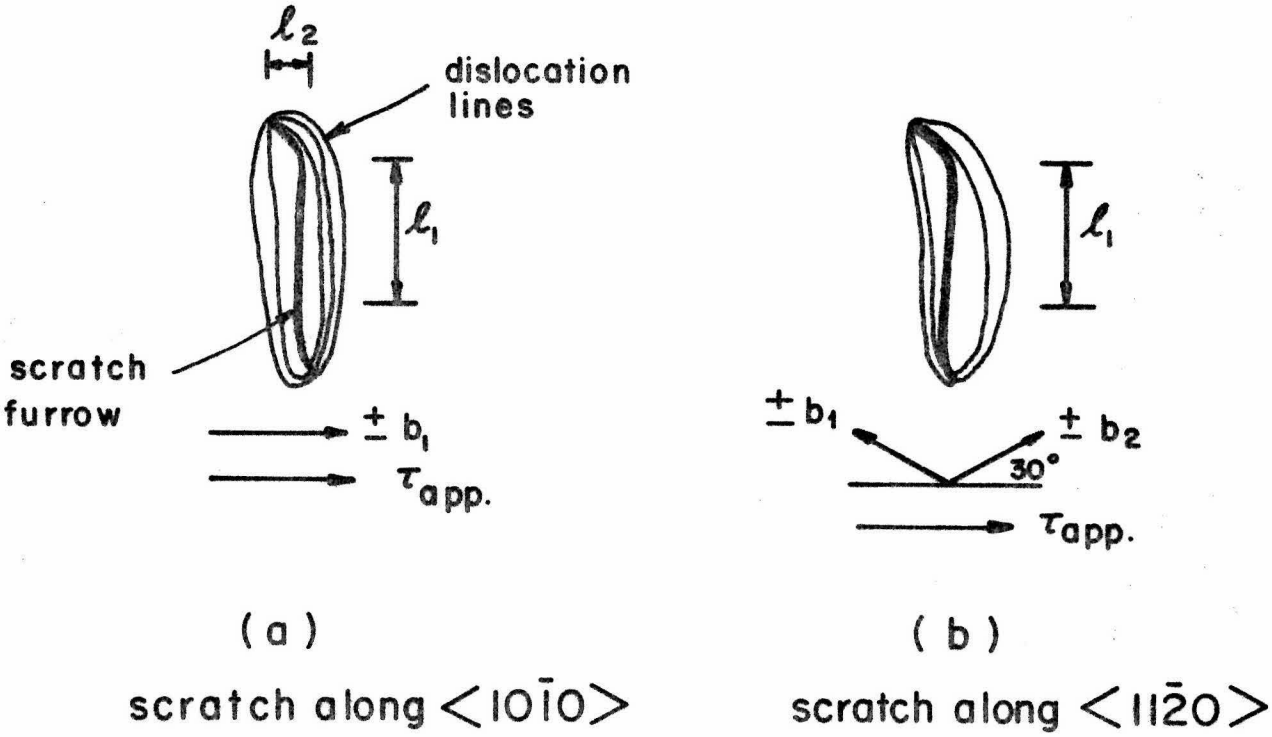

2. Dislocation configuration produced by scratching. In (a) the scratch is a $<10\bar{1}0>$ type producing dislocations of burgers vector $\pm b$ as shown. The segments along ℓ_1 are predominantly of edge orientation and the segments along ℓ_2 are predominantly screw oriented. In (b) the scratch is a $<11\bar{2}0>$ type producing dislocations of burgers vectors $\pm b_1$ and $\pm b_2$ as shown. The displacements of segments ℓ_1 were measured in this case. Note that the applied stress is parallel to $\pm b$ in (a) but there is an angle of 30° between both b_1 and b_2 and the applied stress in (b).

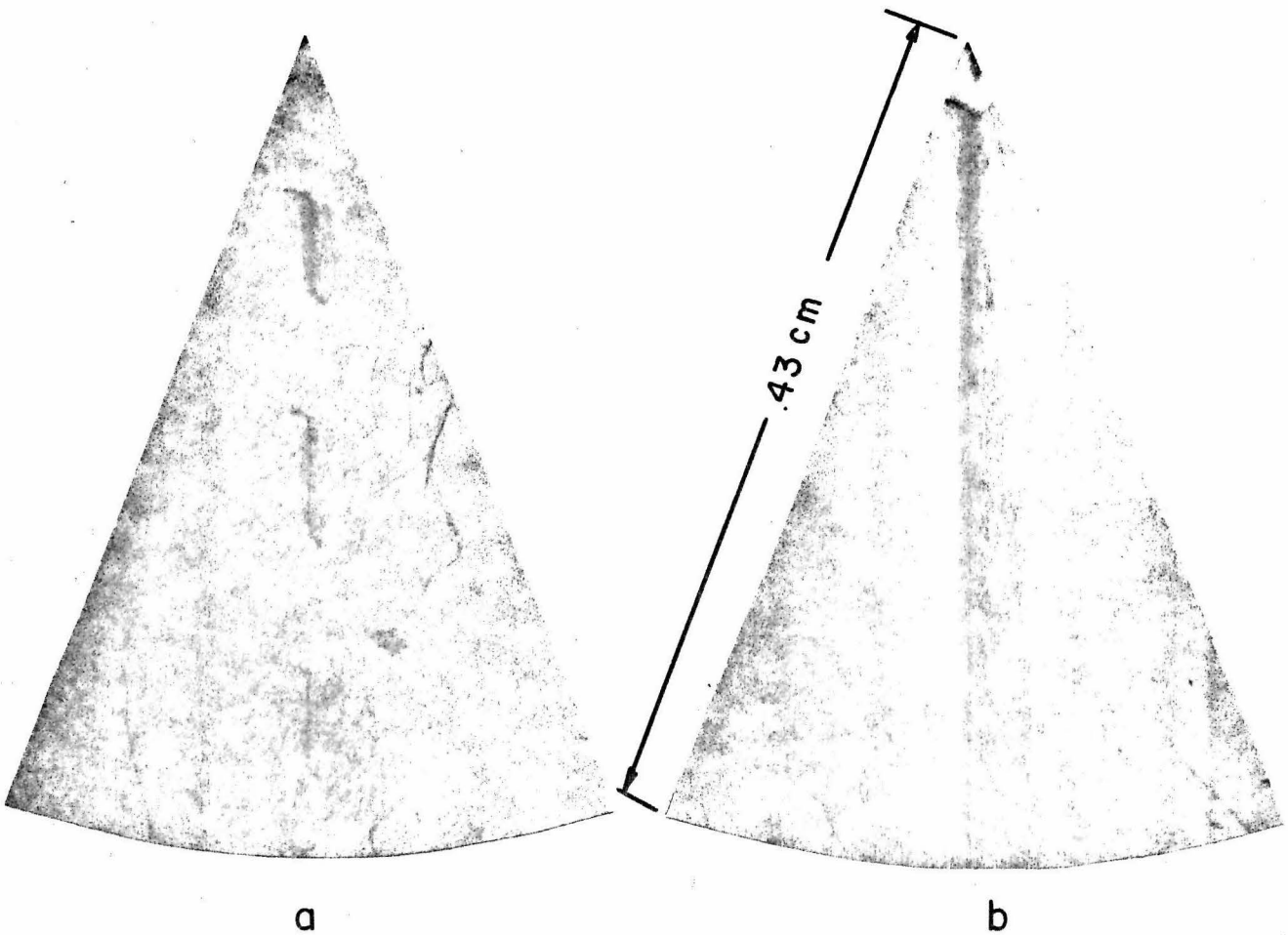

3. (a) Dislocation displacements from a $<10\bar{1}0>$ type scratch. The segments parallel to the scratches are predominantly edge and those perpendicular to the scratches are predominantly screw oriented. (b) Dislocation displacement from a long $<11\bar{2}0>$ type scratch. The applied stress in both cases is horizontal and to the right.

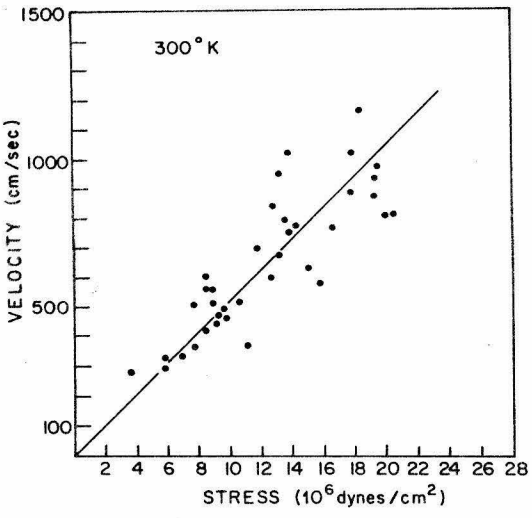

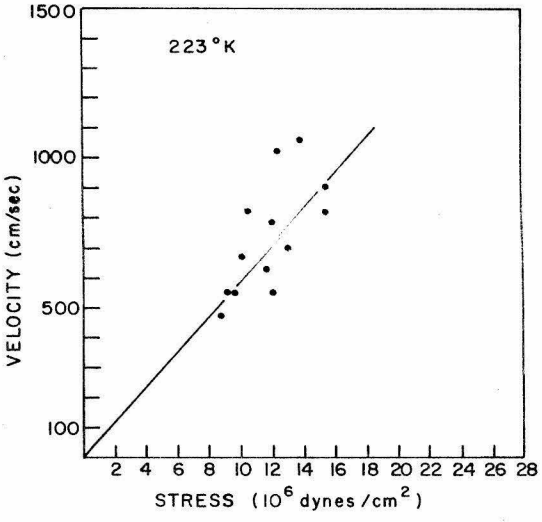

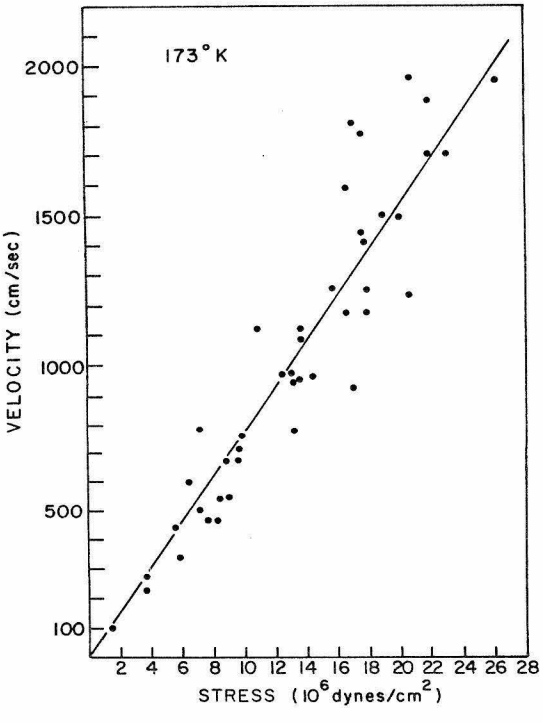

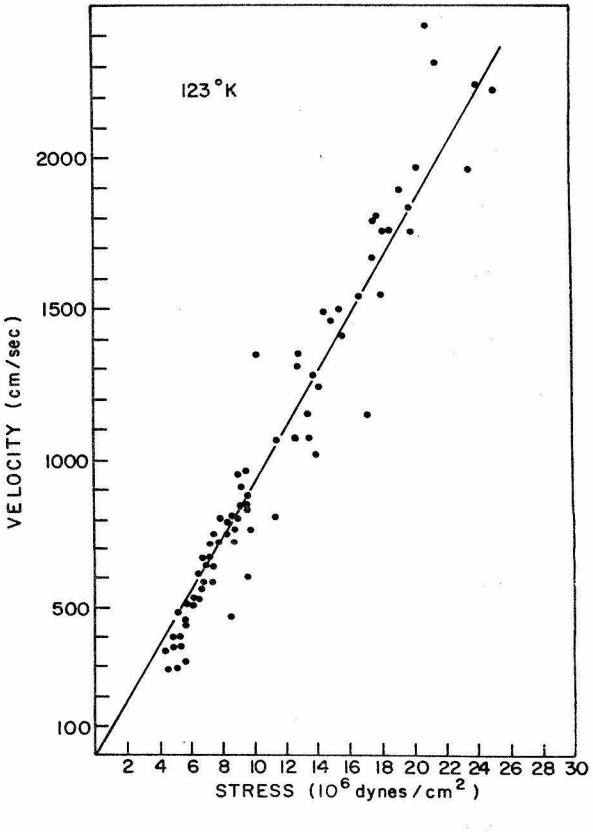

4. Measured edge dislocation velocity as a function of stress at all test temperatures.

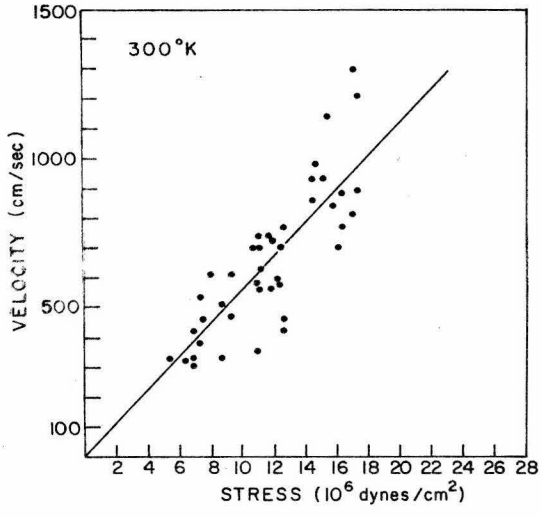

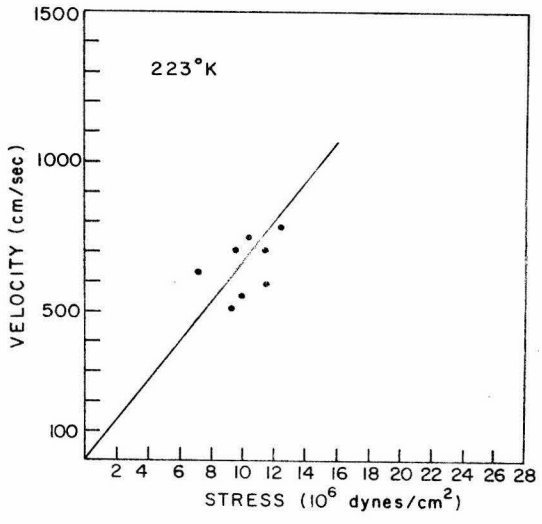

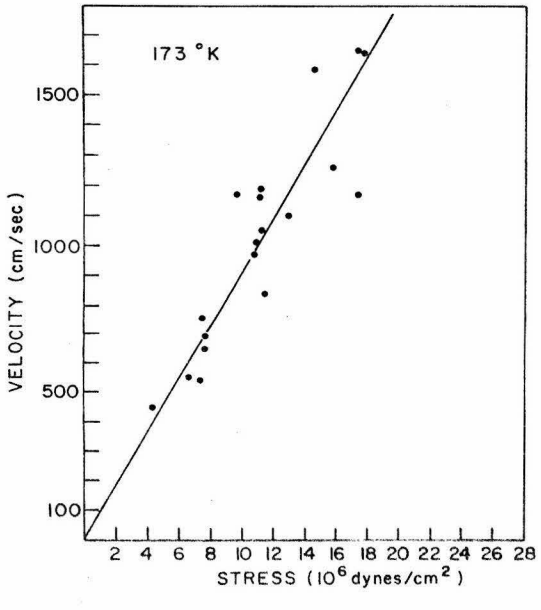

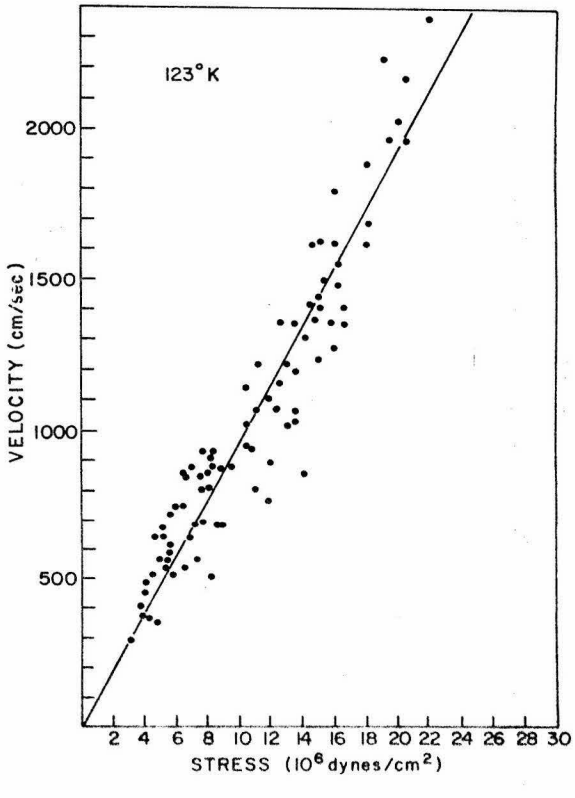

5. Measured mixed dislocation velocity as a function of stress at all test temperatures.

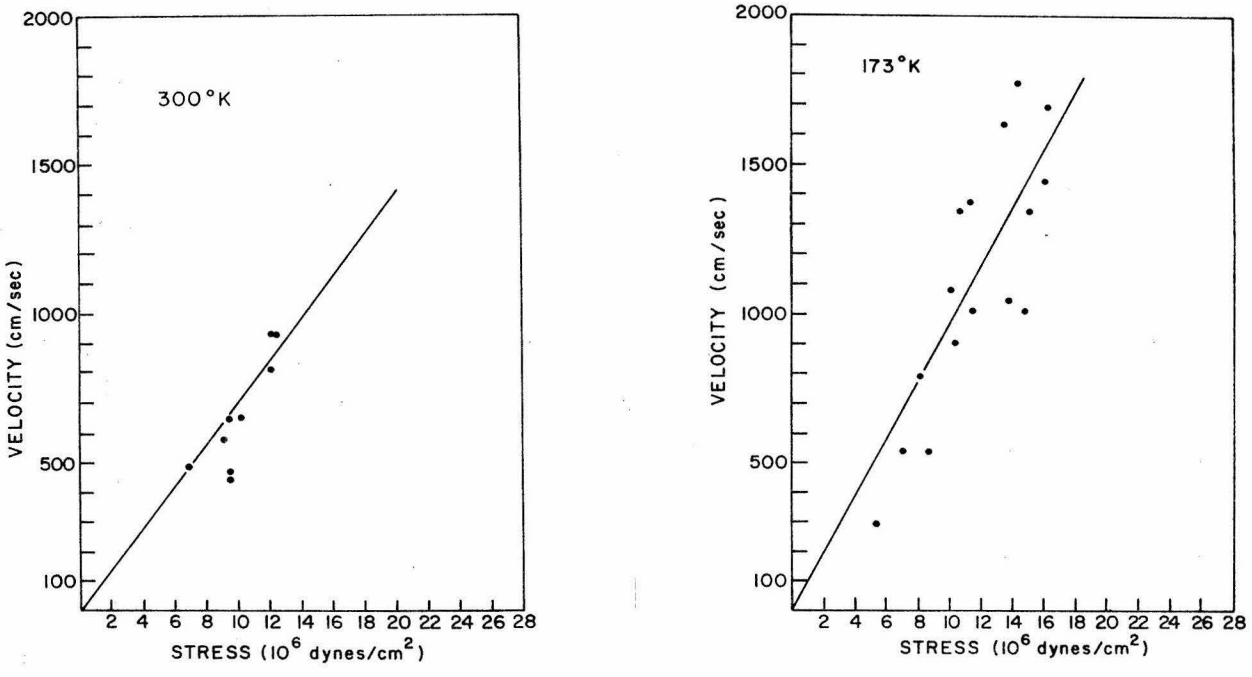

6. Measured screw dislocation velocity as a function of stress at 300°K and 173°K.

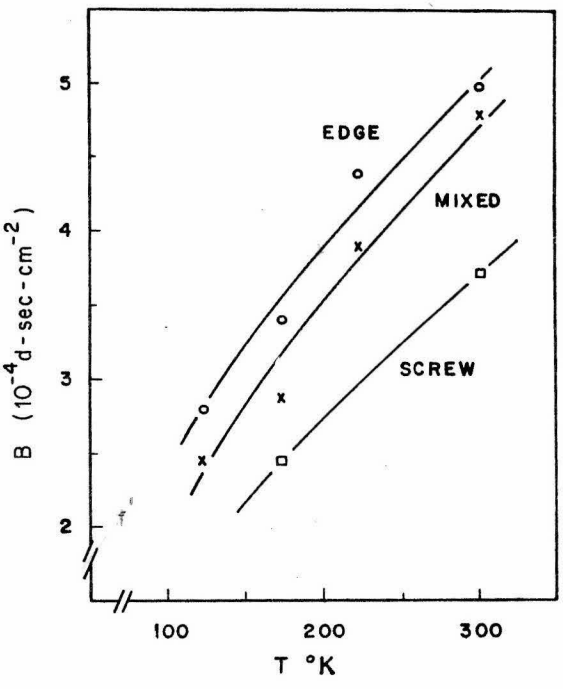

7. Average damping constants versus temperature for edge, screw and mixed dislocations.

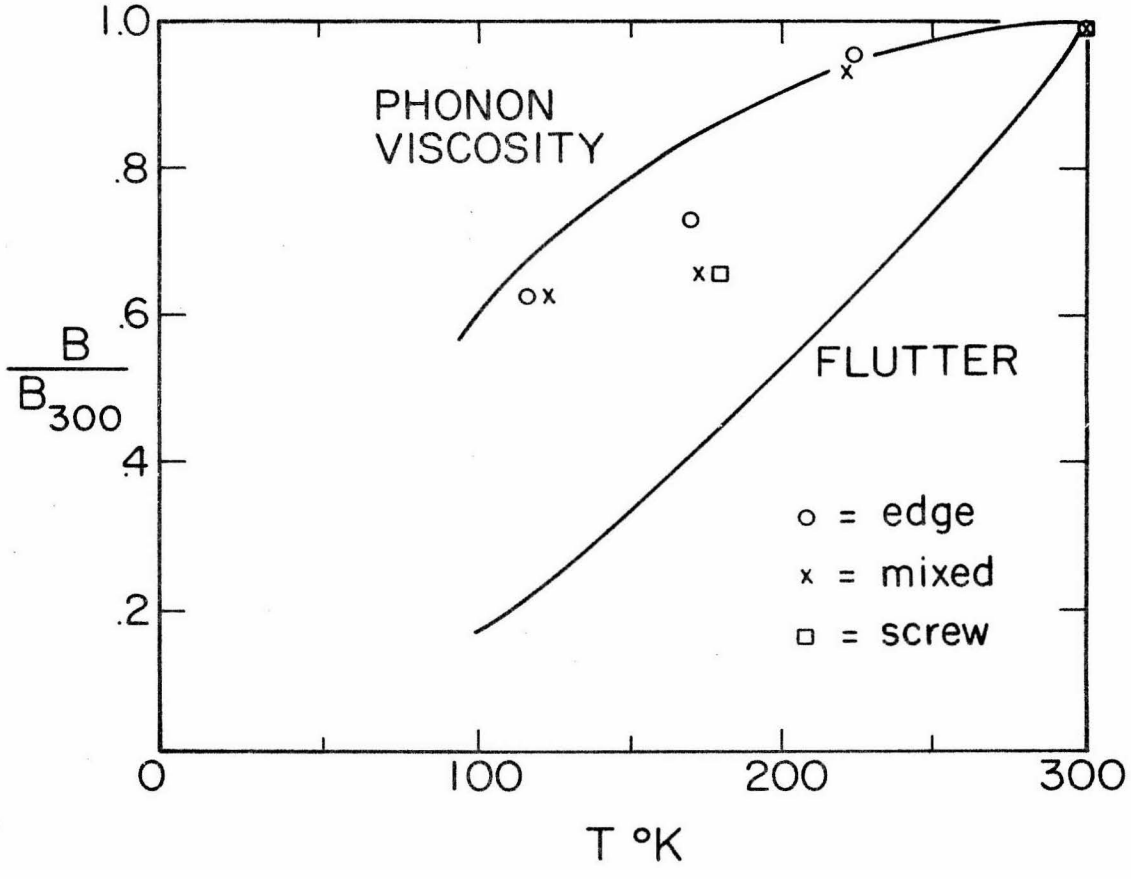

8. Comparison between minimum measured dislocation damping constants and theoretical values. All values normalized to the value at 300°K.